

# A Novel Topology using Cuk Converter in PV Microconverter with Transformerless Injection

A. Ajith<sup>1</sup>, R. Thiyagarajan<sup>2</sup>, A. Nagalingam<sup>3</sup>, Dr. R. Ilango<sup>4</sup>, G. Purushothaman<sup>5</sup>

(B.E(Electrical And Electronics Engineering), M.A.M.School Of Engineering , Tiruchirapalli , Tamilnadu , India) <sup>1,2,3</sup>.

(Prof<sup>4</sup>,Asst Prof<sup>5</sup>, Department Of EEE, M.A.M.School Of Engineering , Tiruchirapalli , Tamilnadu , India ).

**Abstract**— The ‘Cuk derived inverters, employing second-order input and output filters, offer the most efficient, lightweight, and economical solution in the class. This paper presents design and detailed operation of a ‘Cuk derived, common- ground PV microinverter in continuous conduction mode operation. The inverter is shown to be compatible with both linear and nonlinear loads, in stand-alone and grid- connected modes of operation. Optimal design rules of passive components are rigorously derived to ensure attenuation of input voltage ripples arising from the twin effects of switching and double-frequency output power oscillation.

**Index Terms**— Common grounding, inductor design, photovoltaic (PV) inverter, single-stage inverter, transformerless inverter.

## I. INTRODUCTION

POTENTIAL induced degradation of solar photovoltaic (PV) modules is caused by ground leakage current [1], which reduces module power capacity. Leakage current occurs due to common mode voltage ( $V_{cm}$ ), defined as [2], [3]

$$V_{cm} = (V_{an} + V_{bn})/2 \quad (1)$$

in an H-bridge inverter (see Fig. 1). While using unipolar pulse width modulation (PWM),  $V_{cm}$  varies at inverter switching frequency and its multiples. The low impedance offered by the parasitic capacitance ( $C_{pv}$ ), between earth and PV, at these frequencies causes large common mode currents[2],[3].Reduction in the common-mode frequency has been achieved using bipolar

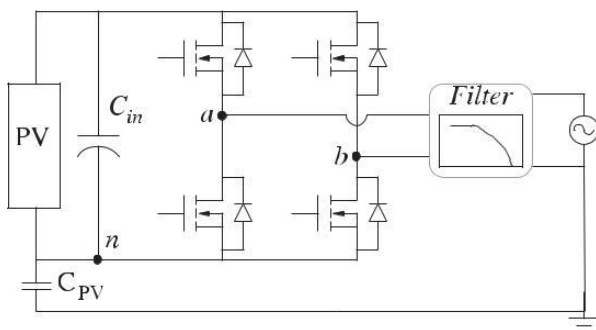


Fig. 1. Leakage current in H-bridge inverter.

PWM [4] or multilevel, neutral-point clamped transformerless topologies [4], [5], or its variant using split inductors [4], [6], [7]. But these offer no voltage boost and hence require series connection of a large number of PV panel so raprior boost stage, both of which degrade the efficiency. H-bridge derived topologies, viz., H-5, H-6, HERIC [8] and HB-ZVR inverters [9] decouple the PV modules from the grid during current freewheeling, when the PV terminals are left floating. For such PV systems, NEC 690.35 stipulates additional ground fault protection. Since the utility neutral is already earthed, this additional protection is inherently obviated in common-grounded PV interface. Though a line-frequency transformer easily achieves double grounding, it makes the system bulky. Topologies using high-frequency transformers [10], [11] suffer from increased losses in the ensuing three-stage power conversion.

## II .EXISTING SYSTEM

Several common-grounded, transformerless topologies have been reported in the literature [12]–[23], which implicitly combine buck–boost and inversion functions. Of these [12], a buck– boost derived topology comprises five active switches and two diodes. In every half cycle, the inductor connections with respect to the output capacitor are reversed by a switch network. A variant [13], based on the same principle, uses an extra diode. However, both are unable to transact reactive power because the series diodes prevent current reversal. Using a pair of coupled inductors, [14] proposes a combination of ‘Cuk and Watkins–Johnson topologies. However, this results in higher currents in the coupled windings, which increases both inductor size and losses. In [15], the circuit topology alternates between a ‘Cuk converter, during the negative half cycle of the output ac voltage, and Zeta converter, for the positive half. Since the plant model changes every half cycle, controller design becomes exceedingly complex.

III. PROPOSED SYSTEM

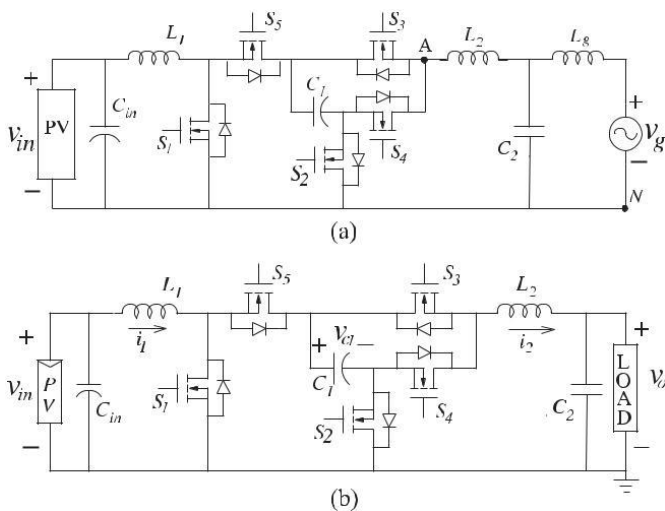


Fig. 2. Inverter schematic. (a) Case I: the inverter in GC mode. (b) Case II: the inverter in SA mode.

An interesting ‘Cuk derived topology [16] achieves cyclic reversal of the connection between the intermediate dc-link capacitor and the output filter, during each half cycle of the output ac voltage. Plant models in the two modes, corresponding to positive and negative output voltages, are similar [24]. Since the inverter retains all the advantages of a ‘Cuk converter, in terms of efficiency, weight and cost [25], it is the better solution in the class. Another variant [17] uses an extra switch in the free-wheeling path of the output filter to reduce conduction loss. In both [16] and [17], use of diodes in series with switches prevent load and source current reversal within each of the modes. Also, the switching sequence is only applicable for unity power factor (UPF) loads, which unnecessarily limits the scope of this promising circuit topology. The major lacuna, however, is in the lack of any justifiable basis for the major performance metrics and design equations which, on some occasions, lead to unacceptable inaccuracies. No analytical or experimental validation of the design rules, for the passive components in the circuit, is provided. This paper presents a modification in the topology of [16], [17], which allows bidirectional power flow, hence

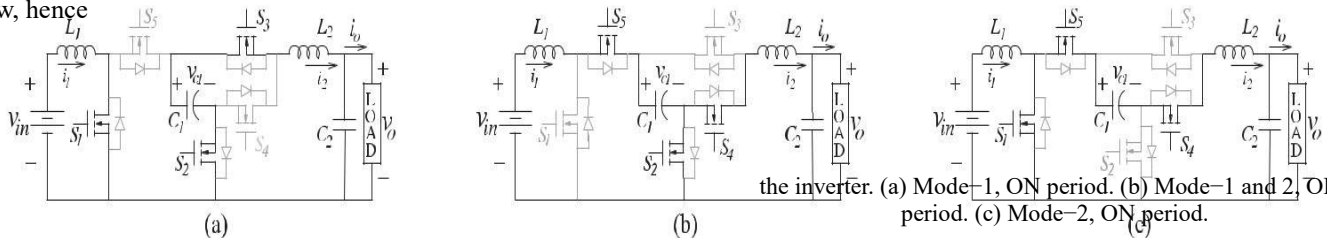


Fig. 3. Circuit diagrams during various operating states of indicated. The actual inductor current direction depends upon the load. Switch current (iS1,...,iS5), inductor current and capacitor voltage waveforms with switching signals, Sg1,...,Sg5 of devices S1,...,S5 respectively, are shown in Fig. 4(a). Since MOSFETs allow bidirectional current flow, the inverter operates in continuous conduction mode under all the load conditions. Considering flux-balance of inductors L1 and L2, steady-

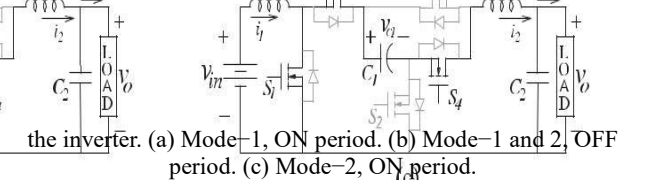
enabling applications involving reactive loads, in addition to UPF loads. It thus includes a thoroughly different switching strategy, apart from justified circuit design rules. Operation of the proposed converter is presented in Section II, where steady-state expressions for inverter states and voltage gain are derived for ideal and nonideal circuit elements. Section III analyzes the effect of double-frequency power oscillation on the input voltage. Section IV systematically lays down well-justified and vastly improved design rules for the inverter components. All analytical conclusions are experimentally validated with a 300-VA laboratory prototype.

IV. CIRCUIT DESCRIPTION AND OPERATION

Circuit diagrams of the inverter in grid connection (GC) and stand-alone(SA) modes are shown in Fig.2. The circuit does not require any common-mode noise filter. The negative conductor and grid neutral (N) are shorted to ensure common grounding hence reduced or no common mode ground current. In GC mode of operation earth connection is provided through grid neutral, whereas in SA mode then negative rail is shorted to avoid runaway potential at the circuit nodes. Composition of circuit elements includes one dc capacitor (C1), five MOSFET (two quadrant) switches (S1 –S5) and second-order input (Cin,L1) and output (C2,L2) filters. Switch S1 is considered as the main switch and the time interval when switch S1 is ON is designated as ON time, the remaining duration of the switching period is designated as OFF time. Depending upon output voltage polarity the inverter operates in two modes, as described below. For ease of explanation, the PV source is replaced by a dc voltage source, Vin.

A. Mode-1 (Vo > 0)

Fig. 3(a) and (b), respectively, show the circuit configurations for the ON and OFF times in this mode of operation. Reference capacitor voltage polarities and inductor current directions are



state duty cycle average (DCASS) [26] of vc1 and vo, over one switching period Ts are obtained as

$$V_{c1}^{(1)} = V_{in} + V_0^{(1)} \quad (2)$$

where D is the steady-state duty cycle. Equating input and output powers, and using (3), DCASS of i1 is expressed as

$$I_1^{(1)} = (V_0^{(1)} / V_{in}) I_0 = (D/1-D) I_0$$

$$\Delta i_1 = (V_{in} DT_s) / L_1 \tag{5}$$

$$\Delta v_{c1} = \{ |I_1^{(1)}| (1-D) T_s \} / C_1 = (|I_0| DT_s) / C_1 \tag{6}$$

$$\Delta i_2 = \{ V_0^{(1)} (1-D) T_s \} / L_2 = (V_{in} DT_s) / L_2 \tag{7}$$

Currents passing through switch pairs (S1,S5) and (S3,S4) are  $i_1$  and  $i_2$ , respectively. During ON period current through S2 is  $i_2$ , whereas during OFF period this is ( $i_1 - i_2$ ). Switches S1 and S3 –S5 are required to block a forward voltage of magnitude equal to  $|v_{c1}|$ . Energy transfer during ON and OFF times depends upon load current direction. Thus two cases are formed, which are as follows.

1) **Case-1a**, ( $I_0 > 0$ ): This is the forward powering mode. Inductor current directions are as shown in Fig. 3(a) and (b).

2) **Case-1b**, ( $I_0 < 0$ ): This is the forward braking mode, which is relevant for reactive loads. Inductor current directions are opposite to those shown in Fig. 3(a) and (b).

**B. Mode-2, ( $V_0 < 0$ )**

Fig. 3(b) and (c) show the circuit configurations for this mode during OFF and ON times, respectively. Switching waveforms of capacitor voltage, inductor current, and switch current are shown in Fig. 4(b). In this mode, S1 and S2 are switched in a complementary manner. Also, throughout the switching period, both S4 and S5 are kept in conduction while S3 is not triggered at all. Assuming switching ripples on the states are small, expressions for DCASS of  $v_o$  and  $v_{c1}$  are

$$V_0^{(2)} = -V_{in} (D / 1-D) \tag{8}$$

$$V_{c1}^{(2)} = (V_{in} / 1-D) = V_{in} - V_0^{(2)} \tag{9}$$

Current  $i_1$  and switching ripple in states ( $\Delta i_1, \Delta v_{c1}, \Delta i_2$ ) are expressed by (4)–(7), which were derived for Mode 1 operation. Currents passing through switch pair (S1,S2) is ( $i_1 - i_2$ ) and that through S4 is  $i_2$ . Switch S5 carries  $i_2$  and  $i_1$  during ON and OFF periods, respectively. The forward blocking voltages of S1, S2, and S3 are identically equal to the magnitude of  $v_{c1}$ . The two cases for different directions of load current are as follows.

1) **Case-2a** ( $I_0 < 0$ ): This is the reverse powering mode and inductor current directions are as shown in Fig. 3(b) and (c).

2) **Case-2b** ( $I_0 > 0$ ): This is the reverse braking mode and arises while feeding reactive loads. Inductor current directions are opposite to those shown in Fig. 3(b) and (c).

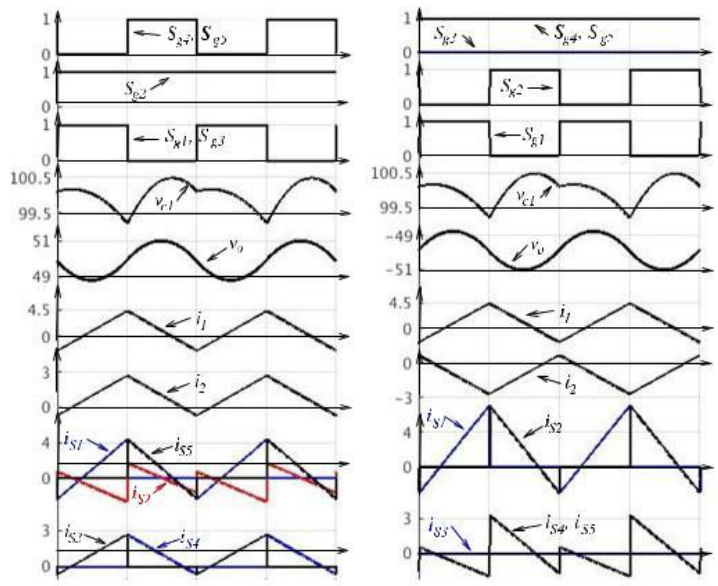


Fig. 4. (a) Switching signals, inductor current, switch current, and capacitor voltage waveforms. (a) Mode-1. (b) Mode-2.

TABLE I  
ON-OFF STATES OF SWITCHES

Switching signal	Mode-1, M=1		Mode-2, M=0	
	On period	Off period	On period	Off period
Sg = Sg 1	1	0	1	0
Sg 2	1	1	0	1
Sg 3	1	0	0	0
Sg 4, Sg 5	0	1	1	1

**C. Design of Inductor L1 and L2**

Design constraints for L1 and L2 are first individually specified. Subsequently, details of engineering optimization to minimize losses are presented.

1) **Constraints for L1:** L1 is required to ensure the switching ripple in  $v_{in}$  is restricted to the allowable maximum,  $\Delta V$  (s) in .

$$\Delta V_{in}^{(s)} \geq (1/2C_{in}) (\Delta i_1/2) (T_s/2) \tag{10}$$

$$L_1 \geq L^{(1)}_{1,min} = V_{in} DT_s^2 / (8C_{in} \Delta V_{in}^{(s)}) \tag{11}$$

$$L_1 \geq L^{(2)}_{2,min} = V_{in} D_{max} T_s / \Delta i_{1,max} (V_{in} T_s / \Delta i_{2,max}) (V_m / V_m + V_{in}) \tag{12}$$

2) **Constraint for L2:** Minimum value of L2 is decided by the maximum allowable switching current ripple. Using (7), and (10)

$$L_2 \geq L_{2,min} = V_{in} D_{max} T_s / \Delta i_{2,max} (V_{in} T_s / \Delta i_{2,max}) (V_m / V_m + V_{in}) \tag{13}$$

TABLE II  
SWITCH RATINGS

Parameters	S1 ,S2	S3 ,S4	S5
Current	$I_m \{1+(v_m /v_{in})\}$	$I_m$	$I_m (v_m /v_{in})$
Voltage	$V_m + v_{in}$	$V_m + v_{in}$	$V_m + v_{in}$

E. Selection of Switches

Minimal switch rating is obviously based on the maximum on-state current and off-state voltage, which are detailed in Section-II. Based on this, Table III lists the selection criteria for all the converter switches.

TABLE III  
SYSTEM PARAMETERS

Inverter Rating	Input 40-100 V dc Output 300VA,110 V
Switching frequency $f_s$	50kHz
$L_1$ and $r_1$	52 $\mu$ H, 2 m $\Omega$
$L_2$ and $r_2$	120 $\mu$ H, 7 m $\Omega$
$C_1$ and ESR	11 $\mu$ F, 8 m $\Omega$
$C_2$ and ESR	3.8 $\mu$ F, 21 m $\Omega$
$C_{in}$ and ESR	2.2 mF, 65 m $\Omega$
$F_s$	100 m $\Omega$
S1 ,S 2 ,S 5 (S3 ,S 4)	IRFP4868 (FDA38N30)

V.SIMULATION AND RESULT

a) Mode-1 ON Period

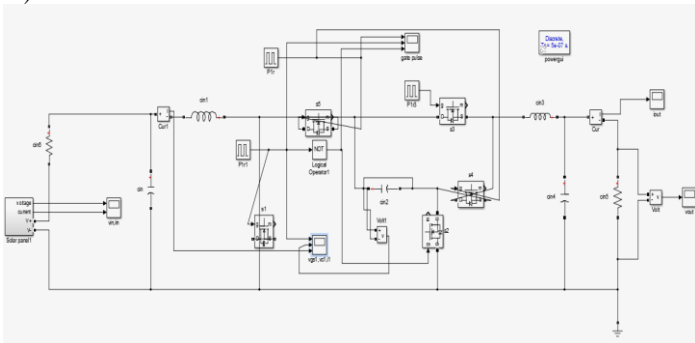


Fig 5. Simulation diagram of mode-1 ON period

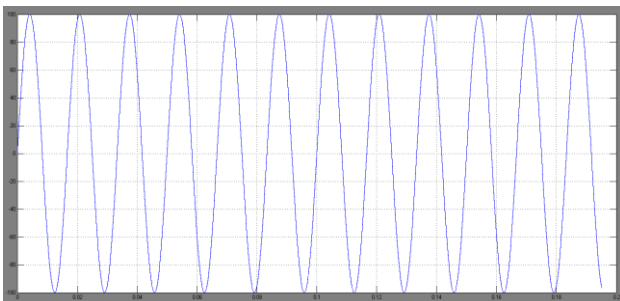


Fig 6. Vout

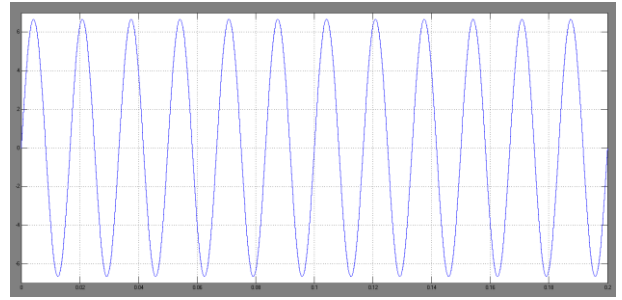


Fig 7. Iout

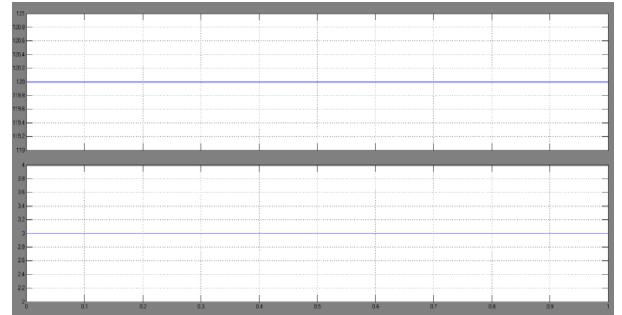


Fig8. Vin Iin

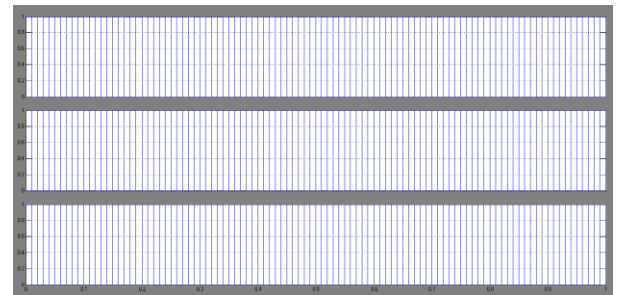


Fig 8. Gate pulse

b) Mode-1, And Mode 2 Off Period

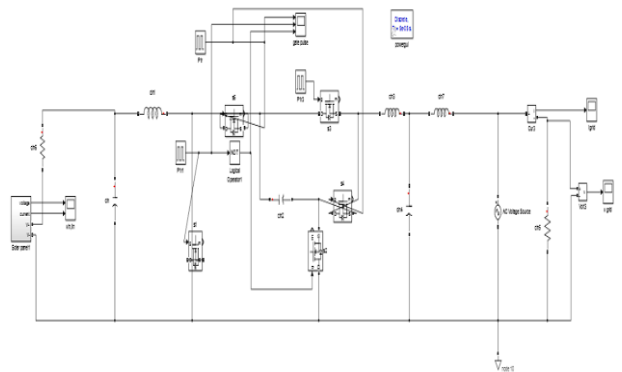


Fig9.Simulation Diagram Of Mode-1 And Mode-2 Off Period

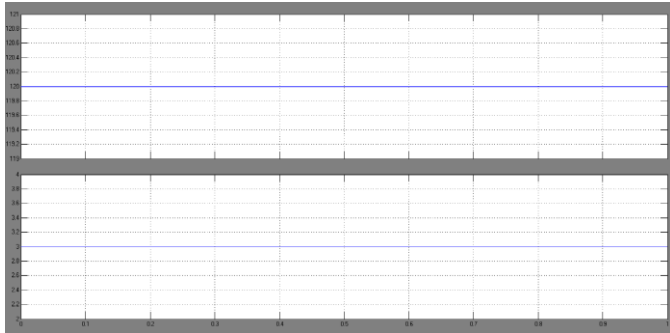


Fig 10. Vin I in

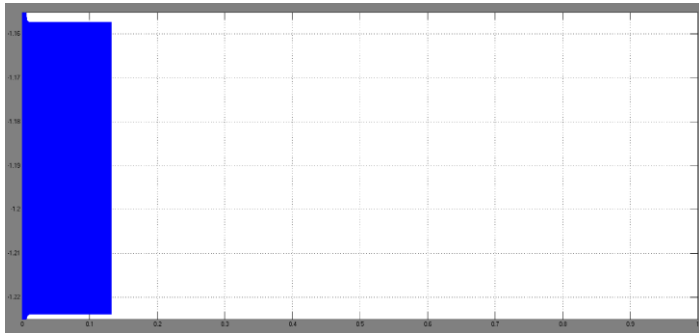


Fig 10. I out

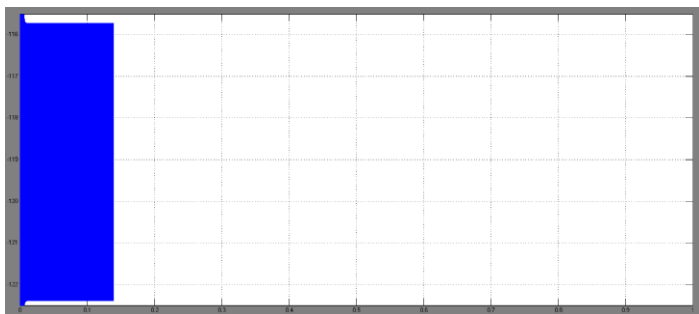


Fig 11. V out

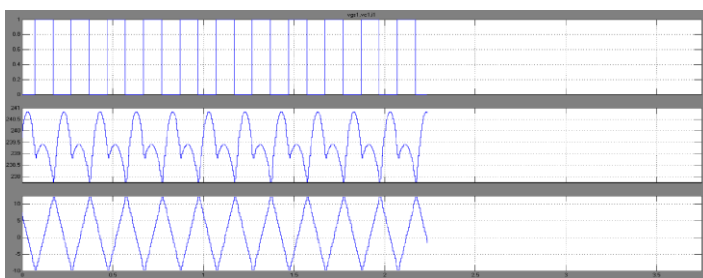


Fig 12. Gate pulse

C) Mode-2 ON period

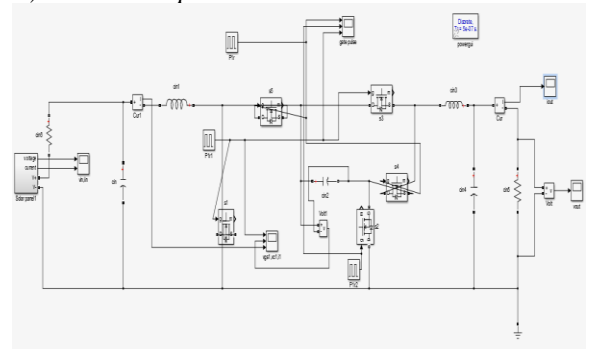


Fig13.simulation diagram of mode-2 ON period

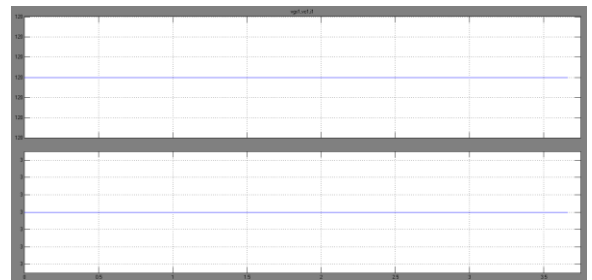


Fig 13.Vin ,lin

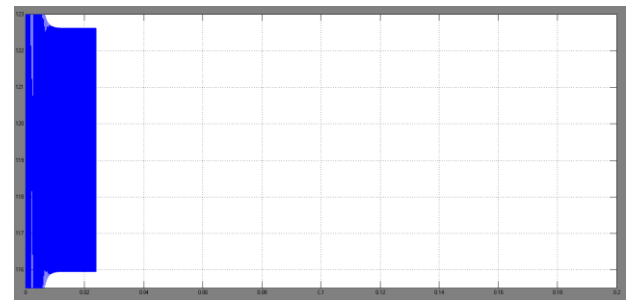


Fig14. V out

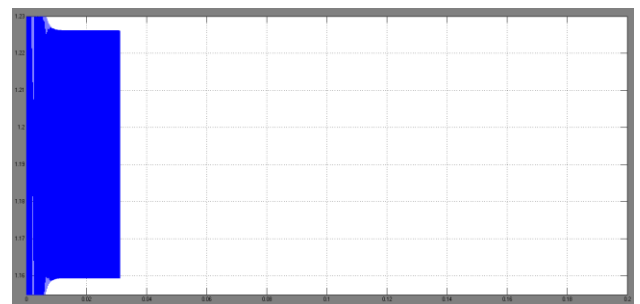


Fig16. I out

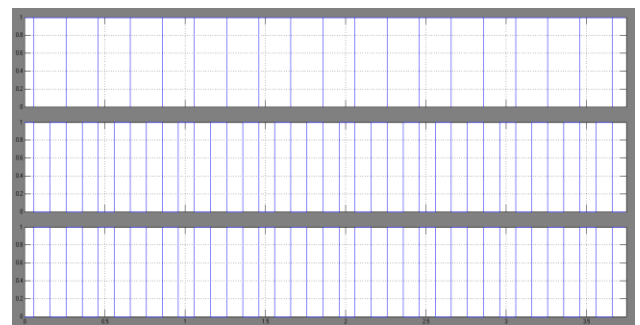


Fig17. Gate pulse

## VI. CONCLUSION

This paper presented the design, operation, and performance of a cost effective, compact, nonisolated, single-stage, single-phase dc-ac PV interface. The topology was specifically designed to practically eliminate common-mode ground leakage current, which has been validated experimentally. All the operating modes, including dead-time operation, were detailed. Optimal design of passive components was described, which consider ripple components due to both switching and double-frequency power oscillations. Additionally, design of all inductors was aimed at maximizing overall efficiency. Output filter design ensured improvement in resonance damping for easing control complexity, while minimally affecting power losses. Inverter performance, with linear/nonlinear loads in SA mode and UPF operation in grid-connected mode, was verified by experiment. Output voltage THD in SA operation and output current.

## REFERENCES

- [1] J. Kapur, K. M. Stika, C. S. Westphal, J. L. Norwood, and B. Hamza-vytechrany, "Prevention of potential-induced degradation with thin ionomer film," *IEEE J. Photovolt.*, vol. 5, no. 1, pp. 219–223, Jan. 2015.
- [2] Y. Tang, W. Yao, P. C. Loh, and F. Blaabjerg, "Highly reliable transformer-less photovoltaic inverters with leakage current and pulsating power elimination," *IEEE Trans. Ind. Electron.*, vol. 63, no. 2, pp. 1016–1026, Feb. 2016.
- [3] D. Barater, G. Buticchi, E. Lorenzani, and C. Concari, "Active common-mode filter for ground leakage current reduction in grid-connected PV converters operating with arbitrary power factor," *IEEE Trans. Ind. Electron.*, vol. 61, no. 8, pp. 3940–3950, Aug. 2014.
- [4] W. Li, Y. Gu, H. Luo, W. Cui, X. He, and C. Xia, "Topology review and derivation methodology of single-phase transformerless photovoltaic inverters for leakage current suppression," *IEEE Trans. Ind. Electron.*, vol. 62, no. 7, pp. 4537–4551, Jul. 2015. [5] Y. Jiao and F. C. Lee, "New modulation scheme for three-level active neutral-point-clamped converter with loss and stress reduction," *IEEE Trans. Ind. Electron.*, vol. 62, no. 9, pp. 5468–5479, Sep. 2015.
- [5] H. Xiao and S. Xie, "Transformerless split-inductor neutral point clamped three-level PV grid-connected inverter," *IEEE Trans. Power Electron.*, vol. 27, no. 4, pp. 1799–1808, Apr. 2012. [7] L. Zhang, K. Sun, L. Feng, H. Wu, and Y. Xing, "A family of neutral point clamped full-bridge topologies for transformerless photovoltaic grid-tied inverters," *IEEE Trans. Power Electron.*, vol. 28, no. 2, pp. 730–739, Feb. 2013.
- [6] N. Vázquez, M. Rosas, C. Hernández, E. Vázquez, and F. J. Perez-Pinal, "A new common-mode transformerless photovoltaic inverter," *IEEE Trans. Ind. Electron.*, vol. 62, no. 10, pp. 6381–6391, Oct. 2015.
- [7] T. Kerekes, R. Teodorescu, P. Rodriguez, G. Vazquez, and E. Aldabas, "A new high-efficiency single-phase transformerless PV inverter topology," *IEEE Trans. Ind. Electron.* vol. 58, no. 1, pp. 184–191, Jan. 2011.
- [8] H. J. Chiu et al., "A module-integrated isolated solar microinverter," *IEEE Trans. Ind. Electron.*, vol. 60, no. 2, pp. 781–788, Feb. 2013.
- [9] S. Kouro, J. I. Leon, D. Vinnikov, and L. G. Franquelo, "Grid-connected photovoltaic systems: An overview of recent research and emerging PV converter technology," *IEEE Ind. Electron. Mag.*, vol. 9, no. 1, pp. 47–61, Mar. 2015.
- [10] 6254 *IEEE TRANSACTIONS ON INDUSTRIAL ELECTRONICS*, VOL. 64, NO. 8, AUGUST 2017
- [11] D. Karschny, "Wechselrichter," German Patent DE196 42 522 C1, Apr. 23, 1998.
- [12] H. Patel and V. Agarwal, "A single-stage single-phase transformer-less doubly grounded grid-connected PV interface," *IEEE Trans. Energy Convers.*, vol. 24, no. 1, pp. 93–101, Mar. 2009.
- [13] V. Gautam, A. Kumar, and P. Sensarma, "A novel single stage, transformer-less PV inverter," in *Proc. IEEE Int. Ind. Tech. Conf.*, 2014, pp. 907–912.
- [14] D. Schekulin, "Transformerless ac. inverter circuit, for coupling photovoltaic systems or wind generator systems, esp. in the low power range, to current networks," German Patent DE197 32 218 C1, Mar. 18, 1999.
- [15] M. Rajeev and V. Agarwal, "Novel transformer-less inverter topology for single-phase grid connected photovoltaic system," in *Proc. 42nd IEEE Int. Photovolt. Spec. Conf.*, 2015, pp. 1–5.
- [16] P. Chamathi, M. Rajeev, and V. Agarwal, "A novel single stage zero leakage current transformer-less inverter for grid connected PV systems," in *Proc. 42nd IEEE Int. Photovolt. Spec. Conf.*, 2015, pp. 1–5.
- [17] J. C. Wu and C. W. Chou, "A solar power generation system with a seven-level inverter," *IEEE Trans. Power Electron.*, vol. 29, no. 7, pp. 3454–3462, Jul. 2014.
- [18] D. Debnath, and K. Chatterjee, "Neutral point clamped transformerless grid connected inverter having voltage buck-boost capability for solar photovoltaic systems," *IET Power Electron.*, vol. 9, no. 2, pp. 385–392, 2016.
- [19] [20] Y. Tang, X. Dong, and Y. He, "Active Buck-Boost inverter," *IEEE Trans. Ind. Electron.*, vol. 61, no. 9, pp. 4691–4697, Sep. 2014.
- [20] [21] H. Hu, S. Harb, N. H. Kutkut, Z. J. Shen, and I. Batarseh, "A single-stage microinverter without using electrolytic capacitors," *IEEE Trans. Power Electron.*, vol. 28, no. 6, pp. 2677–2687, Jun. 2013.
- [21] [22] A. Abramovitz, B. Zhao, and K. M. Smedley, "High-gain single-stage boosting inverter for photovoltaic applications," *IEEE Trans. Power Electron.*, vol. 31, no. 5, pp. 3550–3558, May 2016.
- [22] [23] D. Meneses, O. Garcia, P. Alou, J. A. Oliver, and J. A. Cobos, "Grid-connected forward microinverter with primary-parallel secondary-series transformer," *IEEE Trans. Power Electron.*, vol. 30, no. 9, pp. 4819–4830, Sep. 2015.
- [23] [24] M. Rajeev and V. Agarwal, "Closed loop control of novel transformer-less inverter topology for single phase grid connected photovoltaic system," in *Proc. IEEE Int. Power Energy Conf.*, 2016, pp. 1–7.
- [24] [25] S.M. Cuk, "Modeling, analysis and design of Switching converters," Ph.D. dissertation, Dept. Elect. Eng., California Inst. Technol., Pasadena, CA, USA, 1977.
- [25] Ali, A. Nazar. "Cascaded Multilevel Inverters for Reduce Harmonic Distortions in Solar PV Applications." *Asian Journal of Research in Social Sciences and Humanities* 6.Issue : 11 (2016): 703-715.
- [26] Ali, A. Nazar. "A Single phase Five level Inverter for Grid Connected Photovoltaic System by employing PID Controller." *African journal of Research* 6.1 (2011): 306-315.
- [27] ali, A.Nazar. "A SINGLE PHASE HIGH EFFICIENT TRANSFORMERLESS INVERTER FOR PV GRID CONNECTED POWER SYSTEM USING ISPWM TECHNIQUE." *International Journal of Applied Engineering Research* 10.ISSN 0973-4562 (2015): 7489-7496.
- [28] Ali, A. Nazar. "Performance Enhancement of Hybrid Wind/Photovoltaic System Using Z Source Inverter with Cuk-sepic Fused Converter." *Research Journal of Applied Sciences, Engineering and Technology* 7.ISSN: 2040-7459; (2014): 3964-3970.
- [29] Ali, A. Nazar. "Ride through Strategy for a Three-Level Dual Z-Source Inverter Using TRIAC." *Scientific Research publication* 7.ISSN Online: 2153-1293 (2016): 3911-3921.
- [30] Ali, A. Nazar. "An ANFIS Based Advanced MPPT Control of a Wind-Solar Hybrid Power Generation System." *International Review on Modelling and Simulations* 7.ISSN 1974-9821 (2014): 638-643.
- [31] Nazar Ali, A. "Performance Analysis of Switched Capacitor Multilevel DC/AC Inverter using Solar PV Cells." *International Journal for Modern Trends in Science and Technology* 3.05 (2017): 104-109.
- [32] Ali, A.Nazar. "FPGA UTILISATION FOR HIGH LEVEL POWER CONSUMPTION DRIVES BASED ON THREE PHASE SINUSOIDAL PWM -VVVF CONTROLLER."

- International Journal of Communications and Engineering 4.Issue: 02 (2012): 25-30.
- [33] ali, A.Nazar. "A SINGLE PHASE HIGH EFFICIENT TRANSFORMERLESS INVERTER FOR PV GRID CONNECTED POWER SYSTEM USING ISPWM TECHNIQUE." International Journal of Applied Engineering Research 10.ISSN 0973-4562 (2015): 7489-7496.
- [34] JAIGANESH, R. "Smart Grid System for Water Pumping and Domestic Application using Arduino Controller." International Journal of Engineering Research & Technology (IJERT) 5.13 (2017): 583-588.
- [35] Paul, M., Mano Raja, R., Mahalakshmi, M., Karuppasamyandian, A., Bhuvanesh, and R. Jai Ganesh. "Classification and Detection of Faults in Grid Connected Photovoltaic System."
- [36] Ganesh, Rajendran Jai, et al. "Fault Identification and Islanding in DC Grid Connected PV System." Scientific Research Publishing 7.Circuits and Systems, 7, 2904-2915. (2016): 2904-2915.
- [37] Jaiganesh, R., et al. "Smart Grid System for Water Pumping and Domestic Application Using Arduino Controller." International Journal for Modern Trends in Science and Technology 3.05 (2017): 385-390.
- [38] Kalavalli,C., et al. "Single Phase Bidirectional PWM Converter for Microgrid System." International Journal of Engineering and Technology (IJET) ISSN : 0975-4024 Vol 5 No 3 Jun-Jul 2013.
- [39] Lilly Renuka, R., et al. "Power Quality Enhancement Using VSI Based STATCOM for SEIG Feeding Non Linear Loads. " International Journal of Engineering and Applied Sciences (IJEAS) ISSN: 2394-3661, Volume-2, Issue-5, May 2015.
- [40] Karthikeyan,B. JEBASALMA. "RESONANT PWM ZVZCS DC TO DC CONVERTERS FOR RENEWABLE ENERGY APPLICATIONS ."International Journal of Power Control and Computation(IJPCSC)Vol 6. No.2 – Jan-March 2014 Pp. 82-89@gopalax Journals, Singaporeavailable at :www.ijcns.comISSN: 0976-268X.
- [41] Gowri,N, et al. "Power Factor Correction Based BridgelessSingle Switch SEPIC Converter Fed BLDC
- [42] Motor."ADVANCES in NATURAL and APPLIED SCIENCES. ISSN: 1995-0772 AENSI PublicationEISSN: 1998-1090 <http://www.aensiweb.com/ANAS2016> March 10(3): pages 190-197.
- [43] Ramkumar,R., et al." A Novel Low Cost Three Arm Ac AutomaticVoltage Regulator" ADVANCES in NATURAL and APPLIED SCIENCESISSN: 1995-0772 AENSI PublicationEISSN: 1998-1090 <http://www.aensiweb.com/ANAS2016> March 10(3): pages 142-151.
- [44] Kodeeswaran, S., T. Ramkumar, and R. Jai Ganesh. "Precise temperature control using reverse seebeck effect." In Power and Embedded Drive Control (ICPEDC), 2017 International Conference on, pp. 398-404. IEEE, 2017.
- [45] Subramanian, AT Sankara, P. Sabarish, and R. Jai Ganesh. "An Improved Voltage follower Canonical Switching Cell Converter with PFC for VSI Fed BLDC Motor." Journal of Science and Technology (JST) 2, no. 10 (2017): 01-11.
- [46] Murugesan,S, R. Senthilkumar."DESIGN OF SINGLE PHASE SEVEN LEVEL PV INVERTER USING FPGA."International Journal of Emerging Technology in Computer Science & Electronics, 2016, Vol.20, No.2, pp.207-2012.
- [47] S. Murugesan, C. Kalavalli, " FPGA Based Multilevel Inverter With Reduce Number of Switches For Photovoltaic System", International Journal of Scientific Research in Science, Engineering and Technology(IJSRSET), Print ISSN : 2395-1990, Online ISSN : 2394-4099, Volume 3 Issue 6, pp.628-634, September-October 2017.
- [48] Vikram, A. Arun, R. Navaneeth, M. Naresh Kumar, and R. Vinoth. "Solar PV Array Fed BLDC Motor Using Zeta Converter For Water Pumping Applications." Journal of Science and Technology (JST) 2, no. 11 (2017): 09-20.
- [49] Nagarajan, L. Star Delta Starter using Soft Switch for Low Power Three Phase Induction Motors. Australian Journal of Basic and Applied Sciences, 9(21), 175-178.
- [50] Vinusha, S., & Nagarajan, L. (2015). CURRENT SOURCE INVERTER FED INDUCTION MOTOR DRIVE USING MULTICELL CONVERTER WITH ANFIS CONTROL.
- [51] Nagarajan, L., & Nandhini, S. (2015). AN EFFICIENT SOLAR/WIND/BATTERY HYBRID SYSTEM WITH HIGH POWER CONVERTER USING PSO.
- [52] Subramanian, AT Sankara, P. Sabarish, and R. Jai Ganesh. "An Improved Voltage follower Canonical Switching Cell Converter with PFC for VSI Fed BLDC Motor." Journal of Science and Technology (JST) 2.10 (2017): 01-11.
- [53] Compensator, D. S. (2015). AN ADAPTIVE CONTROL AND IMPROVEMENT OF POWER QUALITY IN GRID CONNECTED SYSTEM USING POWER ELECTRONIC CONVERTERS.
- [54] Sabarish, P., Sneha, R., Vijayalakshmi, G., & Nikethan, D. (2017). Performance Analysis of PV-Based Boost Converter using PI Controller with PSO Algorithm. Journal of Science and Technology (JST), 2(10), 17-24.
- [55] T.Vishnu Kumar, V. Suresh Kumar, T. Sumeet, M.Srimaha "Hybrid Front end Interface DC-DC Converter with ANFIS Based Control of EMS System". International Journal of Scientific Research in Science and Technology, Volume 3, Issue 8, Print ISSN: 2395-6011, 2017.
- [56] T. Vishnu kumar, V. Suresh Kumar, A new approach to front end interface DC-DC converter" International Journal of Multidisciplinary Research and Modern Education (IJMRME) ISSN(online): 2454-6119 Volume I, Issue II, 2015
- [57] V.Suresh kumar, T. Vishnu kumar, A certain investigation for the battery charging system" International Journal of Multidisciplinary Research and Modern Education (IJMRME) ISSN(online): 2454-6119 Vol.1 Issue.1 2015.
- [58] S.Enimai, S.Jayanthi, T.Vishnu kumar Isolated Power System Design Using Modified P&O Technique" Middle-East Journal of Scientific Research 24 (S2): 150-156, 2016, ISSN 1990-9233